Optically heterodyned polarization spectroscopy. Measurement of the orientational correlation function

D. S. Alavi, R. S. Hartman, and D. H. Waldeck

Citation: The Journal of Chemical Physics **92**, 4055 (1990); doi: 10.1063/1.457767
View online: http://dx.doi.org/10.1063/1.457767
View Table of Contents: http://scitation.aip.org/content/aip/journal/jcp/92/7?ver=pdfcov
Published by the AIP Publishing

Optically heterodyned polarization spectroscopy. Measurement of the orientational correlation function

D. S. Alavi, R. S. Hartman, and D. H. Waldeck
Department of Chemistry, University of Pittsburgh, Pittsburgh, Pennsylvania 15260

(Received 30 May 1989; accepted 4 December 1989)

Polarization spectroscopy has been developed as a useful method for the investigation of molecular reorientation in both liquid phase solutions and in the gas phase. This technique has the advantage of measuring a single particle orientational correlation function directly but the disadvantage of averaging over rotation in all electronic states. Described and characterized herein is a variant of this technique, optically heterodyned polarization spectroscopy, which is able to disentangle various contributions to the signal and determine the rotational relaxation of the solute molecule in different electronic states independently. This work also demonstrates the measurement of the normalized value of the orientational correlation function at time zero, $r(0)$, without extensive normalization of laser parameters. Lastly, various technical advantages of the optically heterodyned method are discussed.

INTRODUCTION

Time-resolved polarization spectroscopy as a probe of molecular rotation was first demonstrated by Shank and Ippen[1,2] and has since been used by a variety of workers[3-13] to probe rotational relaxation dynamics in fluid solution. In many cases workers have assumed that rotational relaxation in a single state is observed. This work demonstrates that in the normal configuration used in polarization spectroscopy one necessarily measures a relaxation time which is an average of relaxation in all electronic states. This work further shows how optically heterodyned polarization spectroscopy can be used to selectively probe rotational relaxation in a single electronic state. Such selectivity is necessary in probing the molecular aspects of rotational friction.

In the normal polarization spectroscopy configuration a linearly polarized pump pulse at frequency ω_1 is incident on a sample which contains an isotropic distribution of solute molecules that absorb the light at ω_1. After passage of the pump through the sample the absorbing molecules have an anisotropic distribution of orientations in the excited electronic state and the mirror image of this anisotropy in the ground electronic state. These two anisotropic distributions give rise to a sample which is dichroic and birefringent. Subsequent to the passage of the pump pulse through the sample a linearly polarized probe pulse, at frequency ω_2 and polarized at $\pi/4$ rad from the pump field polarization, is incident on the sample. The transmitted probe pulse is detected through an analyzer polarizer oriented at $-\pi/4$ rad. Because of the anisotropic distribution of absorber molecules in the sample some of the probe intensity is transmitted through this analyzer. As the sample anisotropy relaxes (by rotational relaxation, population relaxation, or other mechanisms) the probe intensity transmitted by the analyzer decreases.

When combined with an independent temporal characterization of the ground state recovery, this technique measures the rotational correlation function

$$r(t) = \tfrac{2}{5}\langle P_2[\boldsymbol{\mu}(0)\cdot\boldsymbol{\mu}(t)]\rangle, \quad (1)$$

where $\boldsymbol{\mu}(t)$ is the orientation of the molecular transition dipole at time t, and $P_2(x)$ is the second Legendre polynomial which describes the spatial shape of the anisotropy produced by dipole absorbers. Note that the two measurements required to determine $r(t)$ in this case need not be normalized, but only their temporal behavior characterized. This is of considerable advantage over fluorescence depolarization and absorption dichroism techniques, which require two separate measurements that must be properly normalized to yield $r(t)$. In practice this can be difficult. In addition, fluorescence depolarization can only monitor rotational relaxation of the emitting excited state. Being a two pulse technique, polarization spectroscopy is also more straightforward than other four wave mixing techniques which require that three pulses be overlapped in the sample. These different techniques have been very ably compared with each other by Myers *et al.*,[13] and more detail can be found in that work. The major limitations these workers find with polarization spectroscopy are given below and can be remedied through optical heterodyning.

Polarization spectroscopy is extremely sensitive to the polarization properties of the probing light field, thus small birefringences in optical components can distort the signal significantly.[5,9] Furthermore, absorption and dispersion properties of different electronic excited states can contribute to the signal and hence an average rotational relaxation rate is observed. In fact, in the simple version of the technique described above there will always be some averaging of all electronic states because the birefringent contribution to the signal is nonresonant. Therefore, in this normal configuration, one generally cannot selectively probe relaxation in a specific electronic state. Lastly, the simple version of the technique measures the square of the rotational correlation function, $r(t)$.

These problems with the technique can be resolved by optically heterodyned detection of the probing light field. This detection scheme has been used by others in nonlinear spectroscopies with continuous lasers[14,15] and in some time resolved studies.[16] In this detection scheme the probe light

 0021-9606/90/074055-12$03.00

field transmitted through the analyzer polarizer (the signal field E_s) is mixed with a second light field (the local oscillator field E_{lo}) at the same optical frequency. The interference term in this mixing process dominates the observed signal if the local oscillator field is made much larger than the signal field,

$$\text{Signal} \propto \text{Re}(E_{lo}^{*} E_s). \quad (2)$$

The work described here characterizes this detection method for time resolved polarization spectroscopy and clearly demonstrates its advantages. In particular, it is shown that the use of heterodyned detection reduces the sensitivity of the detected signal to stray birefringences and imperfections in the optical components. Although difficult to quantify in general, analysis of particular cases indicates improvement by an order of magnitude, and more. Furthermore, it is shown that this detection method can be used to isolate the in-phase (dichroic) and quadrature (birefringent) contributions to the signal. This capability allows for the independent determination of rotational relaxation in different electronic states. Lastly, this detection scheme linearizes the measurement allowing the determination of $r(t)$ with greater precision and improves the signal to noise of the technique allowing the study of weakly absorbing molecules ($\epsilon < 10\,000\ \text{M}^{-1}\ \text{cm}^{-1}$).

The rest of this manuscript is structured as follows. First, the experimental parameters and apparatus are described. Next, a theoretical description of the signal observed in the simple case discussed above and for various heterodyning schemes is presented. This section of the paper also presents the general microscopic model of the solute dynamics used in later sections and draws connections between the description used here and other treatments. The following section of the paper presents simulations of the measured decay curves observed in optically heterodyned polarization spectroscopy and compares these simulations with experimental studies of the polarization spectroscopy signal of a dye molecule, cresyl violet. Subsequently, methods for the determination of $r(0)$ and the relative contribution of dichroism and birefringence are demonstrated. Next the experimental results for cresyl violet are discussed and placed in perspective by comparison with previous literature results. Finally, the results of these studies are summarized and the utility of this technique in the study of molecular rotation is discussed.

EXPERIMENTAL

The experimental arrangement is shown in Fig. 1. The apparatus consists of two independently tunable sources of picosecond laser pulses, a Michelson interferometer for performing pump/probe sampling and a data acquisition system. The general characteristics of such an apparatus have been well documented.[1,3] The specifics of this apparatus follow.

The source of the picosecond laser pulses consists of a single pump laser which is used to drive two dye lasers. The pump laser is a cw modelocked Nd:YAG laser (Spectra Physics Series 3000) which is frequency doubled in a 7 mm KTP crystal (532 nm) and operates at 82 MHz. The angle

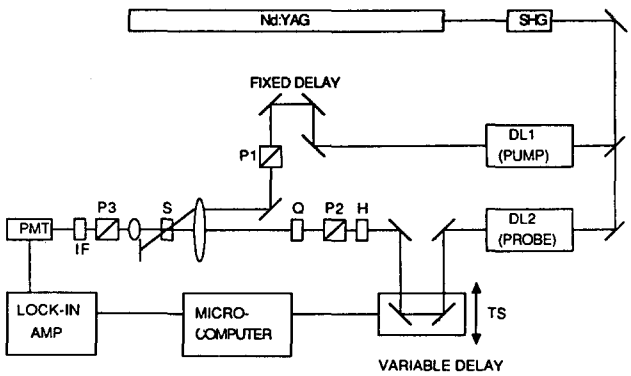

FIG. 1. Schematic diagram of apparatus. SHG = second harmonic generation; DL1, DL2 = dye lasers 1 and 2; P1, P2, P3 = polarizers; H = $\lambda/2$ waveplate; Q = $\lambda/4$ waveplate; S = sample; IF = interference filters; PMT = photomultiplier tube; TS = translation stage.

tuned doubling crystal is mounted outside the laser cavity and is housed in a temperature controlled oven (120 °C). The output from the pump laser is split into two beams and used to synchronously pump two dye lasers (either rhodamine 6G or DCM) which were home built. Output from these independently tunable dye lasers provides the pump and probe pulses for polarization spectroscopy. The dye laser spectra were determined using a 1/2 m Jarrel Ash monochromator in combination with an optical multichannel analyzer (SSR Instruments, model 1205a). Autocorrelation functions of the individual dye lasers were taken on a rotating mirror type autocorrelator (home built)[17] and were typically 6–10 ps FWHM (full width at half-maximum). Cross correlations between the two laser trains provide a measure of the jitter between the dye lasers and supply the instrument function of the apparatus. The method used to cross correlate the two laser pulses was zero background sum frequency generation and in all the experiments discussed the cross correlation profiles were 10 ps FWHM or less. The timing delays for the cross correlations and for the polarization spectroscopy measurements were generated using an interferometer.

The interferometer is of the standard Michelson type. The pump laser pulse travels through the static delay arm and is linearly polarized via polarizer P1. The polarization direction of the pump laser and the propagation direction of the pump laser define the horizontal plane in the laboratory frame. All polarizers are of the Glan Taylor type (model MGTYE08 from Karl Lambrecht Inc.) with extinction ratios (see below) of less than 10^{-6}. The probe laser pulse travels through the variable arm of the interferometer where the path length is varied using a stepping motor controller (Klinger CC1.1) and a 1 μ resolution translation stage (Klinger MT160-250). The probe light is rotated to $\pi/4$ rad by a $\lambda/2$ waveplate and passes through polarizer P2. A $\lambda/4$ waveplate was inserted between polarizer P2 and the sample focussing lens to allow control of the input probe laser polarization. The copropagating pump and probe beams are focused into the sample with a 9 cm focal length lens at an angle of approximately 3 deg from normal. The sample consists of a flowing stream of dye solution from a conventional

dye laser nozzle and has a path length of approximately 1 mm. After the sample the pump laser beam is blocked with an aperture and the probe laser beam is collected with a 7.5 cm focal length lens. The recollimated probe is passed through an analyzer polarizer, P3, followed by a bandpass interference filter and a series of apertures before being detected by a photomultiplier tube (EMI9789QB) or a photodiode (EG&G DT110).

The signal is processed using a lock-in amplifier (PARC 5209) and a microcomputer (Wells American A*2) which also controls the experiment. The signal is detected synchronously by chopping the pump laser at 475 Hz and the probe laser at 846 Hz and monitoring the signal at the difference frequency via the lock-in amplifier. Both the lock-in and the translation stage in the variable delay arm are controlled via the microcomputer. A program using ASYST Scientific Software (MacMillan Inc.) controls the position of the translation stage and records the lock-in signal at each delay setting. The same computer and software are used for the simulation studies and for the fitting of data files.

An important parameter in these studies and this technique is the extinction coefficient of the polarizers. Empirically the extinction coefficient is defined as the light transmitted through a polarizer oriented to minimize light transmission divided by the light transmitted through a polarizer oriented to maximize light transmission—the ratio of blocked to unblocked intensity. This measure provides the ratio of the intensities of the light field in its two perpendicular polarization directions. For ideal polarizers and ideal light polarization this parameter would be zero for linearly polarized light and one for circularly polarized light. The extinction ratio of the probe beam through the two Glan Taylor prism polarizers, P2 and P3, is $<5\times10^{-7}$. With the $\lambda/4$ waveplate and the lenses an extinction ratio of $<3\times10^{-6}$ was obtained.

Other experimental parameters are given below. The sample solutions consisted of the dye molecule cresyl violet perchlorate from Exciton Inc. in absolute ethanol with concentrations ranging from 1×10^{-6} to 3×10^{-4} M. Figure 2 shows the absorption and fluorescence profiles of this dye molecule. The pump laser was 575 nm and had an average power of 50 mW at the sample. The probe laser was 590 nm and had an average power of <5 mW. The laser power affected the overall amplitude of the signal but had no observed effect on its temporal characteristics.

THEORETICAL BACKGROUND

Polarization spectroscopy is a saturation spectroscopy which can be described as a four wave mixing process. An expression for the nonlinear polarization induced in the sample by the pump and probe light fields and its subsequent detection through an analyzer crossed with the incident probe field has been given by Levenson and co-workers[14(a),18] for the continuous wave case and by Myers *et al.*[13] for the time-resolved case. Levenson and co-workers[14] also describe the method of heterodyning the signal and its utility for eliminating background and spurious signals. Their description does not include the orientational relaxation properties of the sample however. Furthermore, they

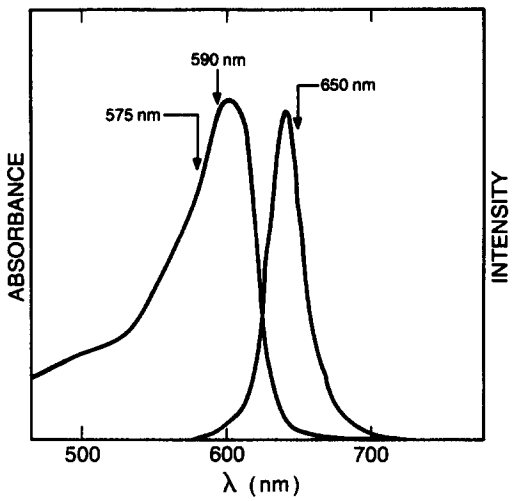

FIG. 2. Absorption and fluorescence spectra of cresyl violet in ethanol.

treat the continuous wave case and all the time permutations of the light fields are present in their treatment. In the experiment described here the probe light field at ω_2 arrives after the pump field at ω_1 has passed through the sample. The distinctions between the nonlinear responses measured by these two different approaches have been outlined by Mukamel *et al.*[19] and by earlier workers.[20] The nonlinear polarization generated in the sample can be computed through the use of the optical Bloch equations[21] and such a procedure has been performed by Band[22] for the polarization spectroscopy experiment described here.

Although Band[22] finds a general expression for the nonlinear polarization, it is most useful to immediately focus on a five state model of the solute molecule for which he solves the optical Bloch equations. In this model there are three electronic states which are explicitly treated and excited vibrational levels are explicitly included in the ground and first excited electronic states. By assuming that vibrational relaxation within an electronic state is rapid, this complex system is reduced to an effective three state system (see Fig. 3). This three state system does not explicitly include vibrational relaxation rates although those effects can be incorporated and have been discussed both by Band[22] and by Laubereau.[8] The

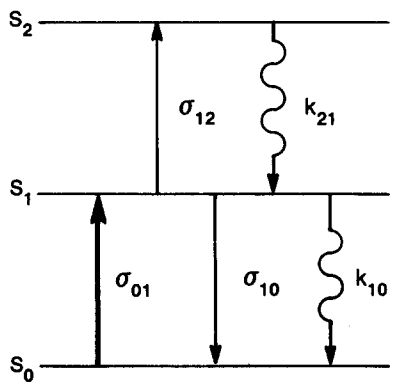

FIG. 3. Effective three state system for the solute molecule. The σ_{ij} couplings are radiative and the k_{ij} couplings are nonradiative.

three state system treats the longer time dynamics (i.e., rotational relaxation) and does include important effects such as excited state absorption and population kinetics. The treatment described here departs from the point of these coupled equations for the population kinetics and follows closely the earlier treatment of Cross *et al.*[6]

As outlined by Cross[6] and Band[22] the pump light will be treated as linearly polarized and defines the laboratory z axis while the propagation direction of the pump beam defines the laboratory y axis (see Fig. 4). Initially (before arrival of the pump pulse), the sample is assumed to be described as an isotropic distribution of dipole absorber molecules. After passage of the pump pulse the sample molecules are described by population distributions in all electronic states which are given by the following expressions

$$N_{\parallel}^{(i)}(\boldsymbol{\mu}^{ij},t) = \int d\boldsymbol{\Omega} f^{(i)}(\boldsymbol{\Omega},t) P_{\parallel}(\boldsymbol{\Omega},\boldsymbol{\mu}^{ij}), \tag{3}$$

$$N_{\perp}^{(i)}(\boldsymbol{\mu}^{ij},t) = \int d\boldsymbol{\Omega} f^{(i)}(\boldsymbol{\Omega},t) P_{\perp}(\boldsymbol{\Omega},\boldsymbol{\mu}^{ij}), \tag{4}$$

where $N_{\parallel}^{(i)}(\boldsymbol{\mu}^{ij},t)$ and $N_{\perp}^{(i)}(\boldsymbol{\mu}^{ij},t)$ are the effective Beer's law concentrations of molecules in state i for probe light polarized parallel and perpendicular to the pump polarization, respectively. The function $f^{(i)}(\boldsymbol{\Omega},t)$ is the probability distribution for finding a molecule in state i with its molecular axes at the Euler angles $\boldsymbol{\Omega}$ with respect to the lab frame at time t, and $P_{\parallel,\perp}(\boldsymbol{\Omega},\boldsymbol{\mu}^{ij})$ is the probability that a molecule oriented at $\boldsymbol{\Omega}$ will interact with parallel or perpendicular probe light through the transition dipole $\boldsymbol{\mu}^{ij}$, which couples state i to state j with the cross section σ_{ij}. Although the treatment described herein is general and applies equally to the case of N excited state levels as treated by Cross,[6] for simplicity and clarity the three state model in Fig. 3 is used. In this limit the populations are given by Eqs. (5) through (10):

$$N_{\parallel}^{(2)}(\boldsymbol{\mu}^{2j},t) \approx 0, \tag{5}$$

$$N_{\perp}^{(2)}(\boldsymbol{\mu}^{2j},t) \approx 0, \tag{6}$$

$$N_{\parallel}^{(1)}(\boldsymbol{\mu}^{1j},t) = \tfrac{1}{3}K^{(1)}(t)[1 + 2r^{(1)}(t,\boldsymbol{\mu}^{1j})], \tag{7}$$

$$N_{\perp}^{(1)}(\boldsymbol{\mu}^{1j},t) = \tfrac{1}{3}K^{(1)}(t)[1 - r^{(1)}(t,\boldsymbol{\mu}^{1j})], \tag{8}$$

$$N_{\parallel}^{(0)}(\boldsymbol{\mu}^{0j},t) = \tfrac{1}{3}K - \tfrac{1}{3}K^{(1)}(t)[1 + 2r^{(0)}(t,\boldsymbol{\mu}^{0j})], \tag{9}$$

$$N_{\perp}^{(0)}(\boldsymbol{\mu}^{0j},t) = \tfrac{1}{3}K - \tfrac{1}{3}K^{(1)}(t)[1 - r^{(0)}(t,\boldsymbol{\mu}^{0j})]. \tag{10}$$

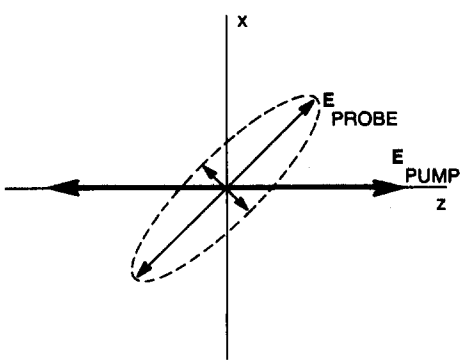

FIG. 4. Axis system for the laboratory frame of reference. The linearly polarized pump defines Z and the probe may be elliptically polarized.

In these equations K is the total absorber concentration, $K^{(1)}(t)$ is the population of the first excited state at time t, and

$$r^{(1)}(t) = \frac{N_{\parallel}^{(1)}(t) - N_{\perp}^{(1)}(t)}{K^{(1)}(t)}, \tag{11}$$

$$r^{(0)}(t) = \frac{N_{\parallel}^{(0)}(t) - N_{\perp}^{(0)}(t)}{-K^{(1)}(t)}. \tag{12}$$

Equation (11) is the standard definition for $r(t)$, agrees with Eq. (1) for any excited state, and will have the expected value of 0.4 at $t = 0$. The modification in Eq. (12) for the ground state expression is necessary for agreement with Eq. (1) and the correct normalized value at $t = 0$.

At this point the treatment departs from the earlier treatment of Cross.[6] In particular, the probe light has components

$$E_{\parallel} = E\cos\psi\exp(i\delta), \tag{13}$$

$$E_{\perp} = E\sin\psi\exp(-i\delta). \tag{14}$$

In Eqs. (13) and (14) E is real and E^2 represents the total probe intensity. For $\delta = 0$ this reduces to linearly polarized probe light at an angle ψ with respect to the pump polarization. For $\psi = \pi/4$ and $|\delta| < \pi/4$, this describes elliptically polarized light with its major axis at $\pi/4$ rad and eccentricity $|\tan(\delta)|$. The analyzer behind the sample is oriented at an angle θ with respect to the pump polarization. Following the Jones matrix procedure described earlier,[5,6] a general expression for the transmitted intensity T is found,

$$T = E^2|S_{\parallel}\cos\psi\cos\theta\exp(i\delta) + S_{\perp}\sin\psi\sin\theta\exp(-i\delta)|^2, \tag{15}$$

where $S_{\parallel}$ and $S_{\perp}$ are the elements of the sample Jones matrix.[6] Assuming the small signal limit and expanding the exponentials to first order yields Eqs. (16) and (17),

$$S_{\parallel} = \exp\left(-\frac{\sigma_{01}\,dK}{6}\right)\left[1 + \frac{d\sigma K^{(1)}(t)}{6} + \frac{dK^{(1)}(t)r(t)}{3} + \frac{i\phi(t)}{2}\right], \tag{16}$$

$$S_{\perp} = \exp\left(\frac{-\sigma_{01}\,dK}{6}\right)\left[1 + \frac{d\sigma K^{(1)}(t)}{6} - \frac{dK^{(1)}(t)r(t)}{6} - \frac{i\phi(t)}{2}\right], \tag{17}$$

where

$$\sigma = \sigma_{01} - \sigma_{12} - \sigma_{10}, \tag{18}$$

$$r(t) = \sigma_{01}r^{(0)}(t,\boldsymbol{\mu}^{01}) - \sigma_{12}r^{(1)}(t,\boldsymbol{\mu}^{12}) - \sigma_{10}r^{(1)}(t,\boldsymbol{\mu}^{10}), \tag{19}$$

$$\phi(t) = \frac{2\pi d}{\lambda_0}C_1(n_s)\sum_{i=0}^{2}\mathrm{Tr}(\boldsymbol{\alpha}^{(i)})r_{\alpha}^{(i)}(t)K^{(i)}(t). \tag{20}$$

Note that in Eqs. (16)–(20), σ_{ij} is not the usual absorption cross section, but is larger by a factor of 3. The phase delay $\phi(t)$ represents the photoinduced birefringence which arises from the difference in the anisotropy of the polarizability in ground and excited states of the solute. This term has been discussed by a variety of previous workers.[5,6,23] The birefrin-

gence interacts nonresonantly with the probe polarization and produces a signal which is sensitive to all electronic states. In these equations d is the sample thickness, λ_0 is the wavelength of probe light, $\alpha^{(i)}$ is the polarizability tensor in electronic state i, $C_1(n_s)$ is given by Cross[6] and accounts for the polarization of the solvent (n_s is the solvent's index of refraction). Although some generality is lost, it is worthwhile to consider four limiting cases for the signal.

The first case is that of a linear polarized probe at $\pi/4$ rad and the analyzer crossed with the input probe polarizer (i.e., $-\pi/4$ rad). Then expression (15) reduces to

$$T \propto S_{ps} = G\frac{E^2}{4}\exp\left(\frac{-\sigma_{01}\,dK}{3}\right) \times\left\{[\phi(t)]^2+\left(\frac{dK^{(1)}(t)r(t)}{2}\right)^2\right\}, \tag{21}$$

where G accounts for the detector response. In the limit that the excited state lifetime is long compared to rotational relaxation [i.e. $K^{(1)}(t)=$ constant] the signal is proportional to $r(t)$ squared. However, if the analyzer is not oriented at $-\pi/4$ rad but deviates from that value by $\delta_D \ll 1$, the transmission is given by the expression

$$T = \frac{E^2}{4}\exp\left(\frac{-\sigma_{01}\,dK}{3}\right)\left|\frac{dK^{(1)}(t)r(t)}{2}+i\phi(t) + \delta_D\left[2+\frac{d\sigma K^{(1)}(t)}{3}+\frac{dK^{(1)}(t)r(t)}{6}\right]\right|^2. \tag{22}$$

This expression has a term quadratic in $r(t)$ and a term linear in $r(t)$. It is this sensitivity of the signal to polarization that previous workers[5,9] have discussed. The extra term which is linear in the anisotropy $r(t)$ is the heterodyned term and is of much utility. By adjusting the analyzer this term can be made much larger than the quadratic term and dominates the signal over a fairly wide range of analyzer orientations. For $1 \gg \delta_D \gg \phi(t)$ or $\sigma dK^{(1)}(t)$ and neglecting the constant (removed by chopping) and higher order terms, the signal is

$$S_{\mathrm{DPS}} = G\frac{E^2}{2}\exp\left(\frac{-\sigma_{01}\,dK}{3}\right)dK^{(1)}(t)r(t)\delta_D. \tag{23}$$

This linear term depends only on the dichroic part of the signal. If the probe wavelength is chosen to be resonant with only one of the electronic states then the anisotropy of that state alone will be probed. In the limit shown here the local oscillator field is in fact given by

$$E_{\mathrm{lo}} = \delta_D E\exp\left(\frac{-\sigma_{01}\,dK}{6}\right) \tag{24}$$

and the signal field is given by

$$E_s = \frac{E}{2}\exp\left(\frac{-\sigma_{01}\,dK}{6}\right)\left[\frac{dK^{(1)}(t)r(t)}{2}+i\phi(t)\right]. \tag{25}$$

The higher order terms in Eq. (22) represent modulation of E_{lo} by the pump pulses and can distort the signal if δ_D is made too large. In fact, these terms must be accounted for when $r(0)$ is determined experimentally.

A second case of interest occurs when the probe is elliptically polarized with its major axis at $\pi/4$ rad and the analyzer is oriented with its transmission axis at $-\pi/4$ rad. If the eccentricity is treated as being small [i.e., from Eqs. (13) and (14) $\delta=\delta_B \ll 1$] then the transmission is

$$T = \frac{E^2}{4}\exp\left(\frac{-\sigma_{01}\,dK}{3}\right)\left|\frac{dK^{(1)}(t)r(t)}{2}+i\phi(t) + i\delta_B\left[2+\frac{d\sigma K^{(1)}(t)}{3}+\frac{dK^{(1)}(t)r(t)}{6}\right]\right|^2. \tag{26}$$

This configuration selects out only the birefringent part of the signal field in the linear term. In the heterodyning nomenclature this corresponds to beating the quadrature component of the signal field with the local oscillator field. The local oscillator field corresponds to

$$E_{\mathrm{lo}} = i\delta_B E\exp\left(\frac{-\sigma_{01}\,dK}{6}\right) \tag{27}$$

and the signal field is given by Eq. (25). It is also possible in this limit to make the linear term much larger than the quadratic term by increasing the size of the local oscillator field. The signal is then given by

$$S_{\mathrm{BPS}} = GE^2\exp\left(\frac{-\sigma_{01}\,dK}{3}\right)\phi(t)\delta_B. \tag{28}$$

In this expression it is not possible to extract out the rotational relaxation in individual electronic states because the birefringence is nonresonant. A comparison of the relative sizes of the birefringent component to the dichroic component can be made by dividing Eq. (28) by Eq. (23).

The last two cases of interest allow the effects of rotation to be removed from the signal and $K^{(1)}(t)$ to be measured. These limits have been discussed previously by Beddard *et al.*[9] and by von Jena *et al.*[4] These limits are also useful because they allow the determination of $r(0)$ in an accurate manner. In the third case the probe is chosen to be linearly polarized at an angle of 0.9553 rad from the pump polarization (i.e., at 54.74 deg, the "magic" angle) and the analyzer is oriented along the same direction. The signal in this case is given by

$$S_{\mathrm{magic}} = G\frac{E^2}{3}\exp\left(\frac{-\sigma_{01}\,dK}{3}\right)\sigma\,dK^{(1)}(t). \tag{29}$$

However, the polarization spectroscopy signal has maximum amplitude when the major axis of the probe is $\pi/4$ rad from the pump polarization. Analysis of Eq. (15) shows that orientational effects are removed if $\tan(\psi)\tan(\theta)=2$ (assuming a linearly polarized probe). If the probe light is linearly polarized at $\pi/4$ rad from the pump polarization and the analyzer is oriented at 1.107 rad (63.44 deg, or the "mystic" angle[4]), the resulting signal is given by

$$S_{\mathrm{mystic}} = G\frac{3E^2}{10}\exp\left(\frac{-\sigma_{01}\,dK}{3}\right)\sigma\,dK^{(1)}(t). \tag{30}$$

These four configurations, all readily obtained in the laboratory, allow the rotational relaxation and population kinetics to be measured in distinct electronic states if a wavelength region exists where one electronic state dominates absorption of the probe light. Another property of interest is the value of the orientational anisotropy at time zero, which for a dipole absorber should be 0.4 (for the ground state). If Eq. (23) is divided by Eq. (30) and only ground state absorption is assumed the following expression is obtained:

$$\frac{S_{\mathrm{DPS}}(t)}{S_{\mathrm{mystic}}(t)} = \frac{\delta_D r^{(0)}(t,\mu^{01})}{0.6}. \tag{31}$$

If the signal is evaluated at zero time delay for the two different analyzer configurations then

$$r^{(0)}(0) = \frac{(0.6)S_{\mathrm{DPS}}(0)}{\delta_D S_{\mathrm{mystic}}(0)}. \tag{32}$$

Thus, $r(0)$ is obtained without the extensive normalization of laser intensities, beam overlap, etc. which are required with fluorescence depolarization or absorption dichroism. The apparatus need only be constant for the time it takes to rotate the analyzer through the appropriate angle. The sensitivity of Eq. (32) to the terms neglected in Eq. (22) is discussed later.

The remainder of the manuscript analyzes these results by computer simulation and by experimental studies of a dye molecule, cresyl violet. To this point the treatment has been general within the context of the three state model assumed at the outset. In the next section particular assumptions are made concerning the population relaxation, $K^{(1)}(t)$, and the rotational relaxation, $r^{(i)}(t)$. In particular, the population kinetics are treated as first order (resulting in an exponential decay law) for $K^{(1)}(t)$. This assumption is appropriate for the dye molecule studied and for many other systems studied on these time scales in fluid solution. The model chosen for the rotational relaxation is that of small step diffusion.[24] Other workers[25] have shown that $r^{(i)}(t)$ is a sum of five (or less) exponentials in this limit. Although the technique measures the correlation function directly, the five exponentials result in a decay profile which is closely approximated by a single exponential whose time constant is a weighted average of the five decay times. The observation of a single exponential decay for $r^{(i)}(t)$ is the most common observation and is used in the modeling here. It should be noted that in some cases two exponentials[26] have been needed to describe $r^{(i)}(t)$.

RESULTS

Simulated decay profiles

Computer simulations of the form of the experimental signal were performed using both Jones vector and Stokes vector/Mueller matrix formalisms.[27,28] The results were the same for either method with one exception. Depolarized light cannot be described in the Jones formalism, so characterization of the effect of depolarization on the signal required the use of the Stokes formalism. In the general scheme, a vector representing the incident probe beam is multiplied by matrices for the input polarizer, $\lambda/4$ waveplate, sample, and analyzer.[5,6] The transformed vector represents the transmitted probe light, from which the signal is extracted. The specifics of the simulation studies are described in the Appendix. In short, the ground state was assumed to be the only absorbing state, and all electronic states were modeled by a single rotational diffusion constant. This approximation allows $r(t)$ to be a single exponential decay and the birefringent contribution to be characterized by a single decay time. Four different cases were considered in the simulation studies.

Case 1: The first simulation was that of a nonheterodyned polarization spectroscopy experiment, with the incident probe polarized at 45° from the pump, and the analyzer at $-45°$. The observed signal had zero background and decayed as a single exponential with a measured decay time $\tau_M = \frac{1}{2}(1/\tau_{\mathrm{OR}} + 1/\tau_F)^{-1}$, in agreement with Eq. (21). A study of the signal size as a function of sample thickness, concentration, and absorption cross section (σ) showed that the optimum signal level behaves as σ^2 and the optimum concentration behaves as $1/\sigma d$. The signal size varied quadratically with the pump pulse energy [also predicted by Eq. (21)], but the pumping level did not effect the optimum concentration or the decay time.

Case 2: The analyzer was rotated by δ_D to simulate heterodyning of the dichroic part of the signal. Figure 5(a) shows the progression of the normalized decay curves as the analyzer was rotated toward the pump polarization [positive δ_{D} in Eqs. (22)–(24)]. Fitting of these curves to a single exponential resulted in decay times ranging from $\tau_M = \frac{1}{2}(1/\tau_{\mathrm{OR}} + 1/\tau_F)^{-1}$ in the nonheterodyned limit to twice that value for sufficiently large δ_D. Notice that Eq. (23) allows a purely dichroic signal to be negative when δ_D is negative. Figure 5(b) shows the progression of the normalized signal from the nonheterodyned case through several "dip" signals to a negative signal which decays exponentially with decay time $\tau_M = (1/\tau_{\mathrm{OR}} + 1/\tau_F)^{-1}$ as δ_D was

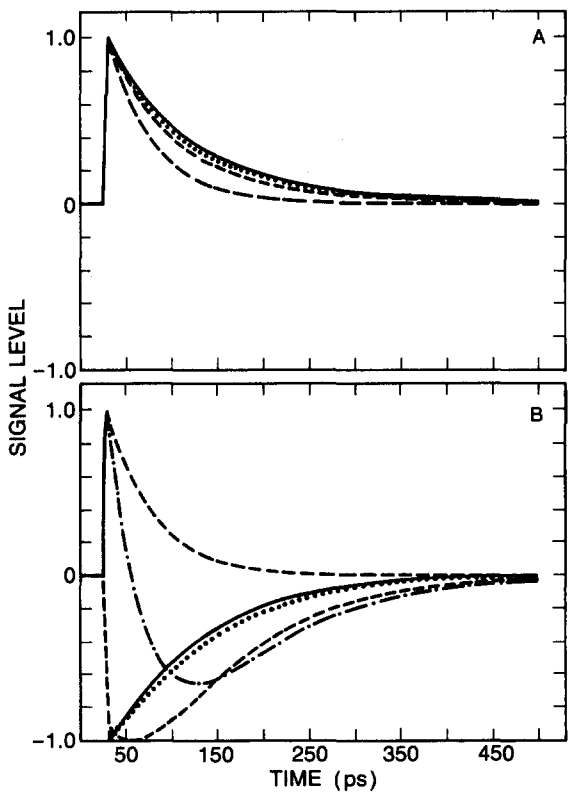

FIG. 5. (a) Simulated decay curves for positive angles of analyzer rotation, (– –) = 0° or nonheterodyned, with a decay time of 50 ps, (---) = 0.2°, (···) = 0.5°, and (—) = 1.0° or fully heterodyned, with a decay time of 100 ps. (b) Simulated decay curves for negative angles of analyzer rotation. (– –) = 0° or nonheterodyned, (–·–·) = −0.1°, (---) = −0.2°, (···) = −0.5°, (—) = −1.0° or fully heterodyned.

made more negative. The dip signal arises because the heterodyned term has a sign opposite that of the nonheterodyned term. Since the two contributions decay at different rates $\{r(t)$ vs $[r(t)]^2\}$ the signal is not monotonic. At longer times, the more slowly decaying heterodyned term begins to dominate the signal, resulting in a change of sign. Once the local oscillator field is made large enough that the heterodyned term dominates at all times the signal is seen to be exponentially decaying.

The dependence of this heterodyned signal on sample length, concentration, and cross section was studied. The dependence of optimum concentration on cross section was identical to the nonheterodyned case. However, the optimized signal level increased linearly with the cross section, not quadratically. The signal is seen to be a maximum at a concentration which is approximately given by

$$\sigma^{\circ}_{\text{pump}}\, dK = \ln 2 \tag{33}$$

in agreement with Eq. (23). This difference in the cross-section dependence of the signal level allows the heterodyned method to be used in the study of more weakly absorbing solute molecules than is the nonheterodyned method.

The simulation studies show that rotating the analyzer so that E_{lo} is approximately $10\times E_s$ yields curves with the proper decay time. For molecules with cross sections in a range from 4×10^{-17} to 4×10^{-16} cm^2 rotation of the analyzer by 0.5 to 1 deg results in a sufficiently large E_{lo}. The decay time τ_M as a function of δ_D rises rapidly from its nonheterodyned value to twice that value, and then increases rather slowly over a fairly wide range (see Fig. 6). This gradual increase in decay time is the result of the higher order terms of Eq. (22), which represent pump modulation of E_{lo} and decay time τ_F. Keeping δ_D less than 1 deg limits the error in the decay times to $<5\%$, which was deemed acceptable for these studies. This source of systematic error can be eliminated by splitting off part of the probe beam before it reaches the sample, and recombining it collinearly with the portion transmitted through the analyzer to provide the local oscillator field. In this way E_{lo} is not modulated by the pump pulse, eliminating higher order terms from Eq. (22).

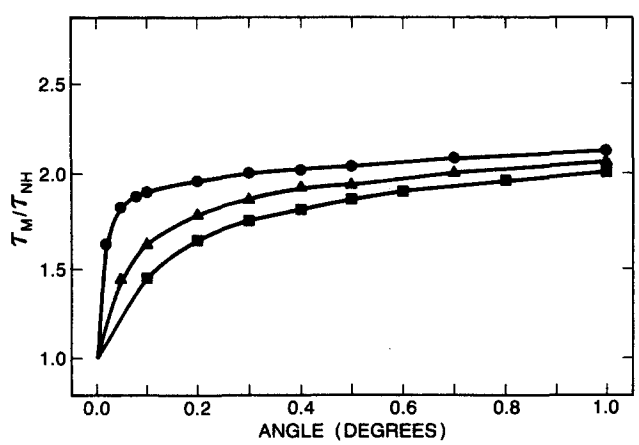

FIG. 6. Decay time (τ_M/τ_{NH}) vs analyzer angle. ●—$\sigma = 0.38$ Å^2; ▲—$\sigma = 1.9$ Å^2; ■—$\sigma = 3.8$ Å^2. All three samples have the same absorbance, so E_{lo} is proportional to analyzer angle.

Case 3: Simulations were performed where the birefringent part of the signal was heterodyned. The procedure required is to rotate the $\lambda/4$ waveplate by a small angle δ_B away from the incident probe polarization, and then tilt the analyzer by the same angle to extinguish the major axis of the resulting elliptical light. The result is a local oscillator field E_{lo} which is $\pi/2$ out of phase with that in the dichroic case. A set of curves totally analogous to those of the dichroic case were obtained. The dips in these curves are caused by interference of the signal phase shift with the probe beam phase shift, and has been discussed by others.[5,9]

Case 4: The simulation was modified to characterize the effect of imperfect optics on the experimental signal. The birefringent contribution to the signal was made infinitely long lived in order to distinguish it from the dichroic contribution. The object of the modification was to evaluate the effect of unwanted birefringence on the signal. A realistic optical system consisting of polarizers and lenses will not have an extinction ratio of zero, but something more on the order of 10^{-6}. The intensity which leaks through the crossed polarizers can arise from one of two sources, either depolarization or stray birefringence. By definition, depolarized light is not coherent with the signal field, and therefore the interference term in Eq. (22) or (26) averages to zero. This reasoning was supported using the Stokes vector formalism which allowed depolarized light to be treated. Birefringence, however, poses greater difficulties. The field which leaks through the polarizers is coherent with the signal field and will heterodyne the birefringent component, distorting the signal. This difficulty can be overcome, and state-specific signals obtained by heterodyning the dichroic part of the signal to an even greater degree. When E_{lo} (dichroic) $>10\times E_{\text{lo}}$ (birefringent), the dichroic part of the signal dominates, and the state-specific signal is recovered. The necessary amount of rotation of the analyzer can be calculated from the measured extinction coefficient of the polarizers as follows:

$$\delta_D(\text{deg}) \gtrsim 600\sqrt{\Gamma}, \tag{34}$$

where Γ is the extinction ratio. Simulations using a modified sample matrix were performed and it was found that the condition in Eq. (34) did indeed yield signals which were dominated by the dichroic contribution.

Measured (experimental) decay profiles

The experimental studies were performed on the dye molecule, cresyl violet in ethanol at room temperature. The temporal behavior of the signal was followed from the nonheterodyned to the fully heterodyned condition and the effect of the samples' optical density (concentration) on the signal was determined. In addition, the usefulness of optical heterodyning for the study of excited states was explored.

Case 1: In the nonheterodyned case, the signal is generated by only that portion of the light field transmitted because of the orientational anisotropy created in the sample by the pump pulse [see Eq. (21)]. A nonheterodyned decay curve for cresyl violet in ethanol ($T = 296$ K) is shown in Fig. 7. The narrow pulse near zero time is the cross correlation of the pump and the probe pulses, hence an indication of the

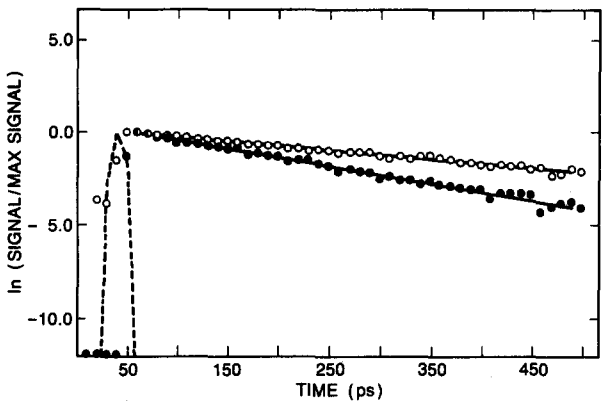

FIG. 7. Experimental decay curves are shown for the both nonheterodyned (●) and heterodyned (○) cases. The smooth curves are a best fit to a single exponential. The dashed curve is the cross correlation of the two laser pulses.

time resolution of the apparatus (9 ps). The decay is fit directly to a single exponential with a lifetime of 108 ps. If both rotational relaxation and the excited state decay are single exponentials then the observed decay time is given by $\tau_M = \frac{1}{2}(1/\tau_{OR} + 1/\tau_F)^{-1}$. If the excited state decay is much slower than the decay of the orientational anisotropy, the rotational decay time can be approximated as twice the observed decay time. Alternatively the excited state decay time can be measured in a separate experiment. It is found that τ_F for cresyl violet in ethanol is 3.39 ns.[29] These observations result in a determination of $\tau_{OR} = 231$ ps for the decay in Fig. 7. This value is in accord with previously reported values for τ_{OR} in ethanol. Table I is a compilation of rotational relaxation times obtained by previous workers and average time constants obtained in this work.

Case 2: For dichroic heterodyning of the signal, the zero angular position of the analyzer was determined by extinguishing the probe pulse (with pump pulse blocked) via the analyzer and the $\lambda/4$ waveplate. As the analyzer was rotated through about 1 deg, decay curves were measured at several points (see Fig. 8). A fully heterodyned decay curve ($\sim 1°$ analyzer rotation) is shown in Fig. 7 and is shown to decay

TABLE I. Rotational relaxation times for cresyl violet in ethanol.

τ_{OR} (ps)	T (K)	Method[a]	Reference
Ground state:			
220 ± 25		AD	30(a)
300 ± 25	294	AD	30(b)
210 ± 20	298	AD	30(c)
223 ± 10	296	PS	5
270	296	AD	30(d)
227 ± 20	296	PS	This work
226 ± 21	296	HPS	This work
Excited state:			
330	294	FD	31(a)
350 ± 14	···	FD	31(c)
243	299	FD	29
265 ± 21	296	HPS	This work

[a] PS: polarization spectroscopy (nonheterodyned), FD: fluorescence depolarization, AD: absorption dichroism, HPS: heterodyned polarization spectroscopy.

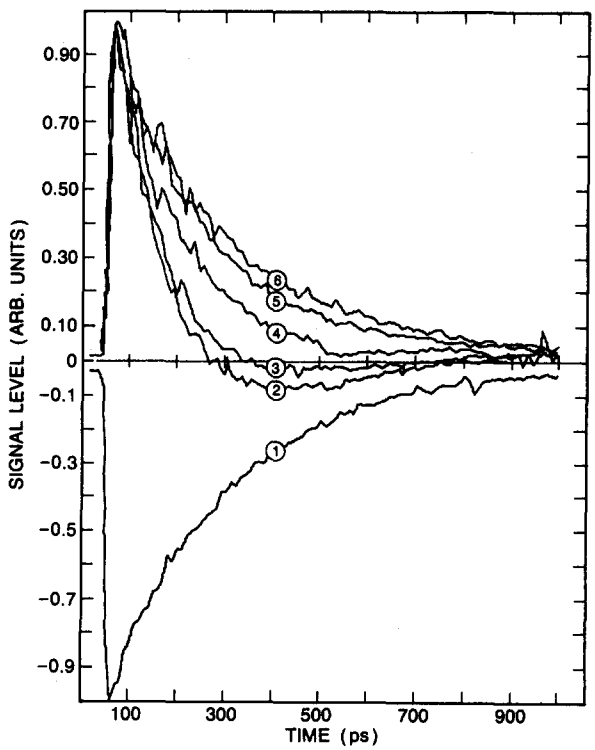

FIG. 8. Measured decay curves are shown for different orientations of the analyzer polarizer. (1) −0.67°; (2) −0.033°; (3) −0.017°; (4) 0.00°; (5) 0.10°; (6) 0.55°.

more slowly ($\tau_M = 209$ ps). This lengthening of the decay profile allows greater temporal precision. Although not necessary in this particular case, this attribute is technically advantageous when the decay is faster. The decay curves in Fig. 7 have been normalized to the same initial value. In fact, the heterodyned signal level is about ten times that of the nonheterodyned signal level.

The curves in Fig. 8 were fit to a single exponential so that a decay time could be associated with the experimental trace. Figure 9 shows a plot of the decay time vs analyzer angle. As was found in the simulations, the observed decay time increases rather sharply with small angles of rotation. As the observed decay time approaches twice the nonheterodyned decay time, the effect of the analyzer rotation on τ_M

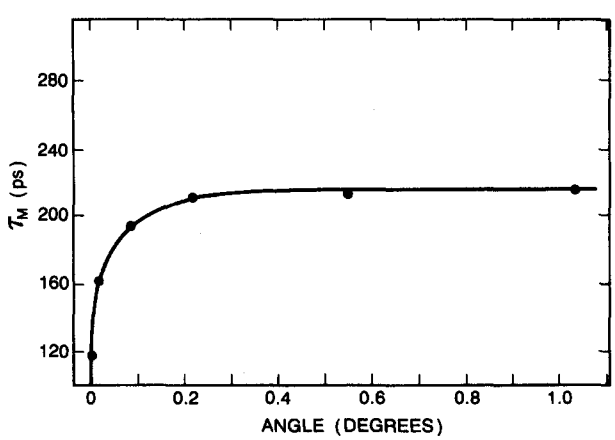

FIG. 9. A plot of decay time vs angle of the analyzer polarizer is shown.

becomes small. Here the plot is nearly asymptotic, resulting in a wide region where τ_M is constant and where its measurement is insensitive to small changes in the analyzer rotation. The small lengthening of decay times with increasing angle apparent in Fig. 9 is analogous to the simulated data in Fig. 6. Those curves in Fig. 8 with dips and the negative curves were generated by rotating the analyzer through negative angles. At large enough negative angles the heterodyned term is dominant and the observed decay time is the same as at large positive angles.

The effect of concentration, ranging from 1×10^{-6} to 3×10^{-4} M, on the heterodyned signal was also explored. In agreement with the simulations, no observable effect of concentration on the fully heterodyned decay times was found. However, the concentration did affect the extent of heterodyning produced for a given analyzer position. Figure 10 shows a plot of τ_M vs analyzer angle for two different concentrations. For the more dilute solution, τ_M approaches the fully heterodyned value with a smaller angle than for the more concentrated solutions. For higher concentrations (3×10^{-5} to 3×10^{-4} M), both nonheterodyned and fully heterodyned decays were obtained. At lower concentrations, reliable nonheterodyned decays could not be obtained, because stray birefringence and imperfect alignment of the analyzer always result in a small local oscillator field which heterodynes the signal. In contrast, fully heterodyned decays were collected for concentrations as low as 1×10^{-6} M. This encouraging result suggests that τ_{OR} for molecules with much lower absorption cross sections than cresyl violet (and correspondingly lower signal levels) might be successfully determined using this method.

Case 3: Heterodyning of the birefringent component of the signal was done in a manner similar to the dichroic heterodyning. These decay curves had the same form as the dichroically heterodyned decays; however, they were usually noisier. A plot of decay time vs $\lambda/4$ waveplate rotation is analogous to that shown in Fig. 9 for the dichroic case.

Excited state studies: The excited state rotational relaxation was studied in an analogous way to that of the ground state. In these experiments, the probe pulse was generated (using DCM as a laser dye) with $\lambda = 650$ nm. This wavelength is outside the absorption range for cresyl violet (see Fig. 2), and thus can interact with only the excited state, causing stimulated emission and/or excited state absorption. The decay curves generated measure the rotational reorientation of the excited state. These curves gave an average value of 265 ± 21 ps which is about 17% longer than the reorientation time for the ground state (226 ± 20 ps).

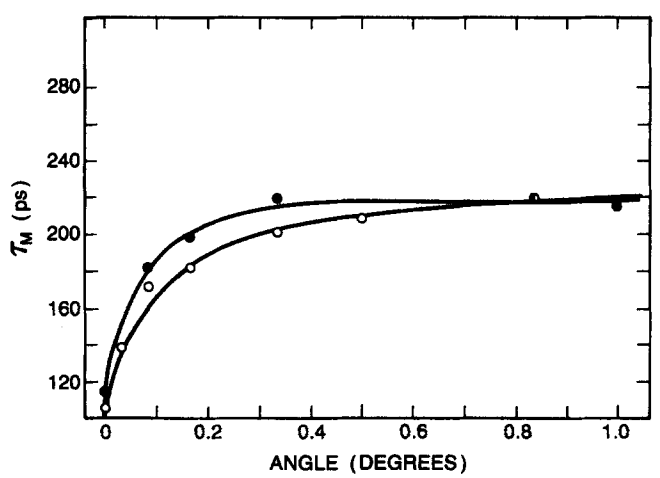

FIG. 10. Plots of measured decay time vs polarizer angle is shown for two different concentrations of cresyl violet in ethanol (7×10^{-5} M = O; 1×10^{-5} M = ●).

The sign of the signal is useful in determining the nature of the interaction of the probe pulse with the excited state. For instance, upon arrival of the pump pulse, molecules with their transition moment oriented horizontally (parallel to the pump polarization) are preferentially excited. If the emission dipole is parallel to the absorption dipole, the photons stimulated by the probe pulse would add to the horizontal component of the probe polarization. The overall effect is to rotate the polarization toward that of the pump pulse, as in the ground state studies, resulting in a positive signal. If instead, the emission dipole is perpendicular to the absorption dipole then the polarization of the probe would rotate away from the pump polarization, and a negative signal would arise.

Determination of $r(0)$

An expression for $r(0)$ is given by Eq. (32). It should be noted that Eq. (32) includes only the heterodyned contribution to the signal. For more strongly absorbing molecules such as cresyl violet, the nonheterodyned contribution can still be a significant part of the observed signal at time zero. Of the other higher order terms, the largest causes an error equal to $2\delta_D$. This term and the nonheterodyned signal level are accounted for by

$$r(0) = \frac{0.6[S_{\mathrm{DPS}}(0) - S_{\mathrm{PS}}(0)]}{\delta_D S_{\mathrm{mystic}}(0)(1+2\delta_D)}. \tag{35}$$

This expression was tested by simulation studies and was found to be accurate to better than 0.5%.

The determination of $r(0)$ required measurements of the nonheterodyned signal level, the heterodyned signal level (at $\delta_D = 1°$) and the signal level at the "mystic angle" discussed earlier. Since the polarization of the probe pulse was 45.0° from the pump, the mystic angle was calculated to be 63.4°. All three measurements were made at zero time and in close succession with no intervening adjustments. Using Eq. (35), this procedure gave an average value of 0.385 ± 0.047 for the ground state. This number is in close agreement with the value of 0.4 predicted by theoretical considerations, and with values obtained from the computer simulation. The $r(0)$ measurement was also made for the excited state and a value of 0.354 ± 0.039 was obtained.

Relative contribution of dichroism and birefringence

The relative contribution of birefringence and dichroism to the signal was also determined. By comparing the signal levels generated by heterodyning both the dichroic and birefringent components, and then adjusting this ratio for the local oscillator field added in each case, the ratio of the two components was calculated. Malus' Law combined

with the small angle approximation allows the assumption that $E_{lo}(D)$ and $E_{lo}(B)$ are proportional to the angles of rotation of the analyzer and $\lambda/4$ waveplate, respectively. Thus, if all other experimental variables remain constant,

$$\frac{E_s(\text{birefringent})}{E_s(\text{dichroic})} = \frac{S_{BPS}\delta_D}{S_{DPS}\delta_B} \tag{36}$$

is obtained from Eqs. (23), (25), and (28). The signal levels for both dichroic and birefringent heterodyning were measured in close succession and with no intervening adjustments of optics or the translation stage. These measurements resulted in an average ratio of 0.8 for $E_s(D)/E_s(B)$ with the probe beam at 590 nm, indicating a nearly equal contribution of dichroism and birefringence to the signal. It is also possible to obtain a spectrum of the dichroic and birefringent signals by tuning the probe laser. Such a study was reported for the dye molecule Oxazine 725.[16(b)] As shown in an earlier study,[5] the absolute value of the birefringent contribution can be used to determine the phase delay, $\phi(t)$. From the phase delay, the value of the anisotropy in polarizabilities of the ground and excited states can be measured. Through the use of Eqs. (20) and (28), this quantity can be determined, although as in the earlier study normalization of laser intensities is required.

CRESYL VIOLET

Although the experimental studies are intended as a demonstration of the technique, some conclusions concerning the rotational relaxation of cresyl violet in ethanol can be drawn. Cresyl violet was chosen for this study because a significant number of different workers have studied its rotational relaxation dynamics[3-5,29-32] and its excited state absorption properties have been studied.[33,34]

Ground state: A compilation of ground state rotational relaxation times of cresyl violet in ethanol are shown in Table I. The average value obtained in this study is 226 ps which is in good agreement with all other work, except that of von Jena and Lessing. The value of this decay time is somewhat higher than expected from a hydrodynamic model with a stick boundary condition.[3-5,28-31] Other workers have invoked specific solute/solvent interactions (hydrogen bonding between the solvent and the dye molecules nitrogen atoms) to explain this discrepancy. More extensive studies are needed to determine the validity of such an explanation. The determination of $r(0)$ to be 0.385 ± 0.047 is in good agreement with the expected value of 0.4 for a dipole absorber. This good agreement also indicates that excited state absorption at the probe wavelength of 590 nm must be small or have a transition dipole collinear with the ground state transition dipole. If the excited state absorption were significant and the dipole oriented differently from the ground state then the overall size of the anisotropy would be reduced [see Eq. (19)], resulting in a value of $r(0)$ less than 0.4. Independent measurements[33,34] indicate that the excited state absorption cross section of cresyl violet is at least 6 times smaller than the ground state absorption cross section at 590 nm. The signal at this wavelength is dominated by the ground state absorption.

Excited state: A compilation of rotational relaxation times for the first electronically excited state of cresyl violet in ethanol are shown in Table I. The average value reported for this work, 265 ps, is in good agreement with unpublished results from this lab using depolarized fluorescence. The values reported here do not agree with those of Beddard,[31] who used fluorescence upconversion to determine $I_{\parallel}(t)$ and $I_{\perp}(t)$. The value obtained in this work is only about 17% longer than the ground state value. The similarity of relaxation rates in the two states is also consistent with the results of nonheterodyned polarization spectroscopy, i.e., the nearly equal contributions of dichroism and birefringence result in a decay time which is one part excited state and two parts ground state. Because the two states have similar time constants, this average relaxation time is not too different from those of the state specific experiment.

Other workers[32] have compared the ground and excited state rotational relaxation times of cresyl violet in other protic solvents and find no evidence of a strong state dependence for the rotational relaxation diffusion coefficients. However, other workers have observed different relaxation times in methanol caused by different emission dipole directions which lead to different combinations of diffusion coefficients.[32] The value of $r(0)$ for the excited state was measured here and found to be 0.354 ± 0.039 indicating only a small change in dipole direction and hence a similar combination of diffusion coefficients. Because the excited state absorption cross section is low (more than five times smaller than the emission cross section[33]), stimulated emission should dominate the contribution to the signal. If so then the value of $r(0)$ lower than 0.4 indicates that the emission dipole is not strictly collinear with the ground state absorption dipole.

The measurement of $r(0)$ in combination with knowledge about the excited state absorption properties of the solute can provide important information concerning the rotational relaxation. If the transition moments have different orientations in the body frame (usually chosen to be the principal axis system of the diffusion tensor), then the observed relaxation time will be composed of different weights of the components of the diffusion tensor,[3,25] resulting in different relaxation times. In these studies it is found that $r(0)$ for the ground state is within the experimental error of being 0.4, the value expected if only the ground state is probed. The observation that the excited state value of $r(0)$ is smaller than 0.4 suggests that the dipole moment may be at a small angle [estimated to be approximately 15 deg using the average value of $r(0)$ given here[25]] to the ground state absorption dipole direction. Such a change could account for the difference in rotational relaxation times observed in the two electronic states. Interestingly the angle between the dipoles and the change in relaxation times are not as large as those observed earlier in methanol.[32] The presence of dielectric friction might also be responsible for the observed difference in relaxation times.[35] Such an explanation would require only a small change in dipole moment between the two electronic states—not an unrealistic expectation. More comprehensive studies are required to address these issues appropriately.

CONCLUSIONS AND SUMMARY

Polarization spectroscopy has the advantage of being a two pulse technique which directly probes the rotational correlation function of the solute, but the disadvantages of no electronic state selectivity and a susceptibility to interference from stray birefringences. This work demonstrates the advantages of optically heterodyned polarization spectroscopy over "normal" polarization spectroscopy in the measurement of orientational correlation functions.

Whereas the signal in the nonheterodyned experiment depends on the anisotropy squared, the heterodyned technique has a signal which is linearly dependent on the anisotropy. As a result the orientational correlation function can be measured with greater temporal precision and with an enhanced signal to noise ratio, allowing more weakly absorbing species to be studied than in the nonheterodyned case.

Whereas the nonheterodyned technique always probes the anisotropy in all electronic states, by heterodyning the in-phase part of the signal a single electronic state can be probed. In particular, the nonresonant part of the signal which arises from pump induced birefringence is masked. This selectivity allows the measurement of rotation times in different excited states as shown here for cresyl violet in ethanol.

Lastly the heterodyning method allows the determination of the anisotropy at zero time, $r(0)$, without extensive normalization of the pump and probe beams. This result is in contrast to fluorescence depolarization and absorption dichroism techniques which require proper normalization to yield not only $r(0)$ but also the temporal behavior of $r(t)$.

ACKNOWLEDGMENTS

This research was supported by NSF Grant No. CHE-8613468. DSA acknowledges the support of a Mellon Predoctoral Fellowship during academic year 1988. We thank E. A. Hoburg for performing the fluorescence depolarization studies of cresyl violet in ethanol.

APPENDIX

Presented here are important specific aspects of the simulation studies. The matrices used in the simulations can be found in Table II. The specific sample matrix elements were [from Eqs. (16)–(20)]

$$S_{\parallel} = \exp\frac{(-\sigma_{01}\,dK)}{6}\exp\left[\frac{\sigma_{01}\,dK^{(1)}(t)}{6} + \frac{\sigma_{01}\,dK^{(1)}(t)}{3}r(t) + \frac{i\phi(t)}{2}\right], \tag{A1}$$

$$S_{\perp} = \exp\left(\frac{-\sigma_{01}\,dK}{6}\right)\exp\left[\frac{\sigma_{01}\,dK^{(1)}(t)}{6} - \frac{\sigma_{01}\,dK^{(1)}(t)}{6}r(t) - \frac{i\phi(t)}{2}\right], \tag{A2}$$

$$K^{(1)}(t) = \frac{I_{\text{pump}}}{dh\nu_{\text{pump}}}\left[1-\exp(-\sigma^{0}_{\text{pump}}\,dK)\right] \times\exp(-t/\tau_F), \tag{A3}$$

$$r(t) = 2/5\exp(-t/\tau_{\text{OR}}), \tag{A4}$$

$$\phi(t) = \phi r(t)\exp(-t/\tau_F), \tag{A5}$$

where I_{pump} is the pump pulse energy per unit area, d is the sample thickness, $h\nu_{\text{pump}}$ is the pump photon energy, $\sigma^{\circ}_{\text{pump}}$ is the absorption cross section of the ground state at the pump wavelength [in Eq. (A3) the usual definition of the absorption cross section is being used], τ_F is the excited state lifetime, and τ_{OR} is the reorientation time. Note that no expansion has been used to approximate the exponentials in Eqs. (A1) and (A2).

The actual experimental parameters used for these studies are $d = 0.05$ cm; $I_{\text{pump}} = 1.5\times10^{-5}$ J/cm^2; $h\nu_{\text{pump}} = 3.3\times10^{-19}$ J; $\tau_F = 500$ ps; and $\tau_{\text{OR}} = 125$ ps. Three different types of simulations were performed using the different parameters given below.

Run	σ (Å^2)	K (M)	K (cm^{-3})	ϕ (rad)
A	0.38	1.66×10^{-3}	3.65×10^{17}	1.7×10^{-3}
B	1.9	3.32×10^{-4}	7.30×10^{16}	8.7×10^{-3}
C	3.8	1.66×10^{-4}	3.65×10^{16}	1.7×10^{-2}

For each σ a value for ϕ was chosen which yielded dichroic and birefringent contributions which were roughly equal. The incident probe beam was of unit intensity. The background transmission was subtracted from the total transmitted intensity to yield the signal. Simulated curves were fit to a single exponential decay law to yield a relaxation time.

TABLE II. Jones (2×2) and Mueller (4×4) matrices used in simulations.

Polarizer (transmission axis at angle θ)	$\lambda/4$ waveplate (fast axis at angle θ)	Sample
$\begin{bmatrix}\cos^2\theta & \cos\theta\sin\theta\\ \cos\theta\sin\theta & \sin^2\theta\end{bmatrix}$	$\begin{bmatrix}\cos^2\theta - i\sin^2\theta & (1+i)\cos\theta\sin\theta\\ (1+i)\cos\theta\sin\theta & \sin^2\theta - i\cos^2\theta\end{bmatrix}$	$\begin{bmatrix}S_{\parallel} & 0\\ 0 & S_{\perp}\end{bmatrix}$
$\begin{bmatrix}1 & \cos2\theta & \sin2\theta & 0\\ \cos2\theta & \cos^2 2\theta & \cos2\theta\sin2\theta & 0\\ \sin2\theta & \cos2\theta\sin2\theta & \sin^2 2\theta & 0\\ 0 & 0 & 0 & 0\end{bmatrix}$	$\begin{bmatrix}1 & 0 & 0 & 0\\ 0 & \cos^2 2\theta & \cos2\theta\sin2\theta & -\sin2\theta\\ 0 & \cos2\theta\sin2\theta & \sin^2 2\theta & \cos2\theta\\ 0 & \sin2\theta & -\cos2\theta & 0\end{bmatrix}$	$\begin{bmatrix}S_{\bullet} & D_{\bullet} & 0 & 0\\ D_{\bullet} & S_{\bullet} & 0 & 0\\ 0 & 0 & \mathrm{Re}(S_{\parallel}^{*}S_{\perp}) & -\mathrm{Im}(S_{\parallel}^{*}S_{\perp})\\ 0 & 0 & \mathrm{Im}(S_{\parallel}^{*}S_{\perp}) & \mathrm{Re}(S_{\parallel}^{*}S_{\perp})\end{bmatrix}$

$$S_{\bullet} = \frac{|S_{\parallel}|^2 + |S_{\perp}|^2}{2};\quad D_{\bullet} = \frac{|S_{\parallel}|^2 - |S_{\perp}|^2}{2}$$

[1] C. V. Shank and E. P. Ippen, *Ultrashort Light Pulses*, edited by S. L. Shapiro, Topics in Applied Physics, Vol. 18 (Springer, New York, 1977).
[2] C. V. Shank and E. P. Ippen, Appl. Phys. Lett. **26**, 62 (1975).
[3] G. R. Fleming, *Chemical Applications of Ultrafast Spectroscopy* (Oxford University, New York, 1986).
[4] H. E. Lessing and A. von Jena, *Laser Handbook*, edited by M. L. Stitch (North-Holland, New York, 1979), Vol. 3.
[5] D. H. Waldeck, A. J. Cross, D. B. McDonald, and G. R. Fleming, J. Chem. Phys. **74**, 3381 (1981).
[6] A. J. Cross, D. H. Waldeck, and G. R. Fleming, J. Chem. Phys. **78**, 6455 (1983).
[7] (a) D. H. Waldeck and G. R. Fleming, J. Phys. Chem. **85**, 2614 (1981); (b) D. H. Waldeck, W. T. Lotshaw, D. B. McDonald, and G. R. Fleming, Chem. Phys. Lett. **88**, 297 (1982); (c) S. K. Kim and G. R. Fleming, J. Phys. Chem. **92**, 2168 (1988); (d) S. H. Courtney, S. K. Kim, S. Canonica, and G. R. Fleming, J. Chem. Soc. Faraday Trans. 2 **82**, 2065 (1986).
[8] (a) D. Reiser and A. Laubereau, Ber. Bunsenges. Phys. Chem. **86**, 1106 (1982); (b) D. Reiser and A. Laubereau, Chem. Phys. Lett. **92**, 297 (1982).
[9] G. S. Beddard and M. J. Westby, Chem. Phys. **57**, 121 (1981).
[10] (a) M. Lee, A. J. Bain, P. J. McCarthy, C. H. Han, J. N. Haseltine, A. B. Smith III, and R. M. Hochstrasser, J. Chem. Phys. **85**, 4341 (1986); (b) A. J. Bain, P. J. McCarthy, and R. M. Hochstrasser, Chem. Phys. Lett. **125**, 307 (1986).
[11] R. M. Bowman, K. B. Eisenthal, and D. P. Millar, J. Chem. Phys. **89**, 762 (1988).
[12] J. B. Clark, A. L. Smirl, E. W. van Stryland, H. J. Mackey, and B. R. Russell, Chem. Phys. Lett. **78**, 456 (1981).
[13] A. B. Myers and R. M. Hochstrasser, IEEE J. Quantum Electron. **22**, 1482 (1986).
[14] (a) M. D. Levenson, *Introduction to Nonlinear Laser Spectroscopy* (Academic, New York, 1982); (b) G. L. Eesley, M. D. Levenson, and W. M. Tolles, IEEE J. Quantum Electron. **14**, 45 (1978); (c) J. J. Song, G. L. Eesley, and M. D. Levenson, Appl. Phys. Lett. **29**, 567 (1976).
[15] A. Owyoung, IEEE J. Quantum Electron. **14**, 192 (1978).
[16] (a) W. T. Lotshaw, D. McMorrow, C. Kalpouzos, and G. A. Kenney-Wallace, Chem. Phys. Lett. **136**, 323 (1987); (b) G. R. Fleming, W. T. Lotshaw, R. J. Gulotty, M. C. Chang, and J. W. Petrich, Laser Chem. **3**, 181 (1983).
[17] Z. A. Yasa and N. M. Amer, Opt. Commun. **36**, 406 (1981).
[18] J. J. Song, J. H. Lee, and M. D. Levenson, Phys. Rev. A **17**, 1439 (1978).
[19] S. Mukamel and R. F. Loring, J. Opt. Soc. Am. B **3**, 595 (1986).
[20] (a) R. W. Hellwarth, Prog. Quantum Electron. **5**, 1 (1977); (b) P. N. Butcher, *Nonlinear Optical Phenomena*, Engineering Experiment Station Bulletin 200 (Ohio State University, Columbus, OH, 1965).
[21] L. Allen and J. H. Eberly, *Optical Resonance and Two-Level Atoms* (Dover, New York, 1975).
[22] Y. B. Band and R. Bavli, Phys. Rev. A **36**, 3203 (1987).
[23] (a) K. B. Eisenthal and K. E. Rieckhoff, J. Chem. Phys. **55**, 3317 (1971); (b) M. F. Yuks, Opt. Spectrosc. **20**, 361 (1966).
[24] (a) P. Debye, *Polar Molecules* (Dover, New York, 1929); (b) W. T. Huntress, Adv. Magn. Reson. **4**, 1 (1970); (c) A. Einstein, *Investigations on the Theory of Brownian Motion* (Dover, New York, 1956).
[25] (a) T. Tao, Biopolymers **8**, 609 (1969); (b) T. J. Chuang and K. B. Eisenthal, J. Chem. Phys. **57**, 5094 (1972); (c) G. G. Belford, R. L. Belford, and G. Weber, Proc. Natl. Acad. Sci. U.S.A. **69**, 1392 (1979); (d) M. Eherenberg and R. Rigler, Chem. Phys. Lett. **14**, 539 (1972).
[26] (a) R. L. Christensen, R. C. Drake, and D. Phillips, J. Phys. Chem. **90**, 5960 (1986); (b) M. D. Barkley, A. A. Kowalczyk, and L. Brand, J. Chem. Phys. **75**, 3581 (1981); (c) P. E. Zinsli, Chem. Phys. **20**, 299 (1977); (d) J. L. Viovy, J. Phys. Chem. **89**, 5465 (1985); (e) H. Labhart and E. R. Pantke, Chem. Phys. Lett. **23**, 482 (1973).
[27] E. Hecht, *Optics* (Addison, Reading, Mass, 1987).
[28] W. S. Bickel and W. M. Bailey, Am. J. Phys. **53**, 468 (1985).
[29] Fluorescence depolarization studies were performed by E. A. Hoburg using the time-correlated single photon counting technique. The particular apparatus used has a time response of 60ps full width at half-maximum and has been reported on previously. See D. M. Zeglinski and D. H. Waldeck, J. Phys. Chem. **92**, 692 (1988) for more details.
[30] (a) D. P. Millar, R. Shah, and A. H. Zewail, Chem. Phys. Lett. **66**, 435 (1979); (b) A. von Jena and H. E. Lessing, *ibid.* **78**, 187 (1981); (c) E. F. G. Templeton and G. A. Kenney Wallace, J. Phys. Chem. **90**, 5441 (1986); (d) A. von Jena and H. E. Lessing, Chem. Phys. **40**, 245 (1979).
[31] (a) G. S. Beddard, T. Doust, and J. Hudales, Nature **294**, 154 (1981); (b) T. Doust and G. S. Beddard, *Picosecond Phenomena III*, edited by K. B. Eisenthal (Springer, New York, 1982); (c) G. S. Beddard, T. Doust, and G. Porter, Chem. Phys. **61**, 17 (1981).
[32] (a) G. J. Blanchard and C. A. Cihal, J. Phys. Chem. **92**, 5950 (1988); (b) G. J. Blanchard, J. Chem. Phys. **87**, 6802 (1987); (c) G. J. Blanchard and M. J. Wirth, *ibid.* **82**, 39 (1985); (d) G. J. Blanchard and M. J. Wirth, J. Phys. Chem. **90**, 2521 (1986).
[33] W. Blau, W. Dankesreiter, and A. Penskofer, Chem. Phys. **85**, 473 (1984).
[34] (a) R. F. Leheny and J. Shah, IEEE Quantum Electron. **11**, 70 (1975); (b) J. Shah and R. F. Leheny, Appl. Phys. Lett. **24**, 562 (1974).
[35] D. Kivelson and K. G. Spears, J. Phys. Chem. **89**, 1999 (1985).